On-Site Meteorological Data and Off-Site Long Term Representativeness

Ludeman In-Situ Uranium Recovery Project

February 2015

Prepared for:

Uranium One Americas, Inc.

Prepared by:

IML Air Science

A division of Inter-Mountain Labs, Inc.

555 Absaraka Street

Sheridan, WY 82801

(307) 674-7506

TABLE OF CONTENTS

1.0 Background

NRC's Request for Additional Information (NRC 2013) stipulated on-site monitoring at Ludeman or a justification for the use of non-site-specific meteorological data. Uranium One Americas subsequently installed an on-site meteorological monitoring station. This station has been collecting hourly average data for over a year. For the purpose of this report, the baseline monitoring year is considered to extend from February 1, 2014 through January 31, 2015. The criteria and procedure for siting the Ludeman met station are described in Appendix B. An instrument audit report is contained in Appendix C. The following report includes an on-site baseline year meteorology characterization, a comparison of on-site to originally referenced off-site wind characteristics, and an off-site demonstration of the long-term representativeness of the baseline monitoring year. Appendix A contains an in-depth evaluation of statistical methods potentially applied to this demonstration.

2.0 Baseline Year Meteorology Summary

Instrument specifications for the Ludeman meteorological monitoring station are presented in Appendix B. Parameters monitored include horizontal wind speed and direction, standard deviation of horizontal wind speed (sigma theta), ambient temperature at heights of 2 and 10 meters, precipitation, relative humidity, barometric pressure and solar radiation. Following is a brief summary of the meteorological conditions observed during the baseline monitoring year.

2.1 Temperature

Figure 1 shows monthly average temperatures ranging from 19° F in February to 71° F in July. Daily high temperatures averaged 32° F in February and 84° F in July. Figure 2 shows an average diurnal temperature swing of 27° F in summer and 10° F in the winter.

Figure 1 – Ludeman Site Monthly Average Temperatures

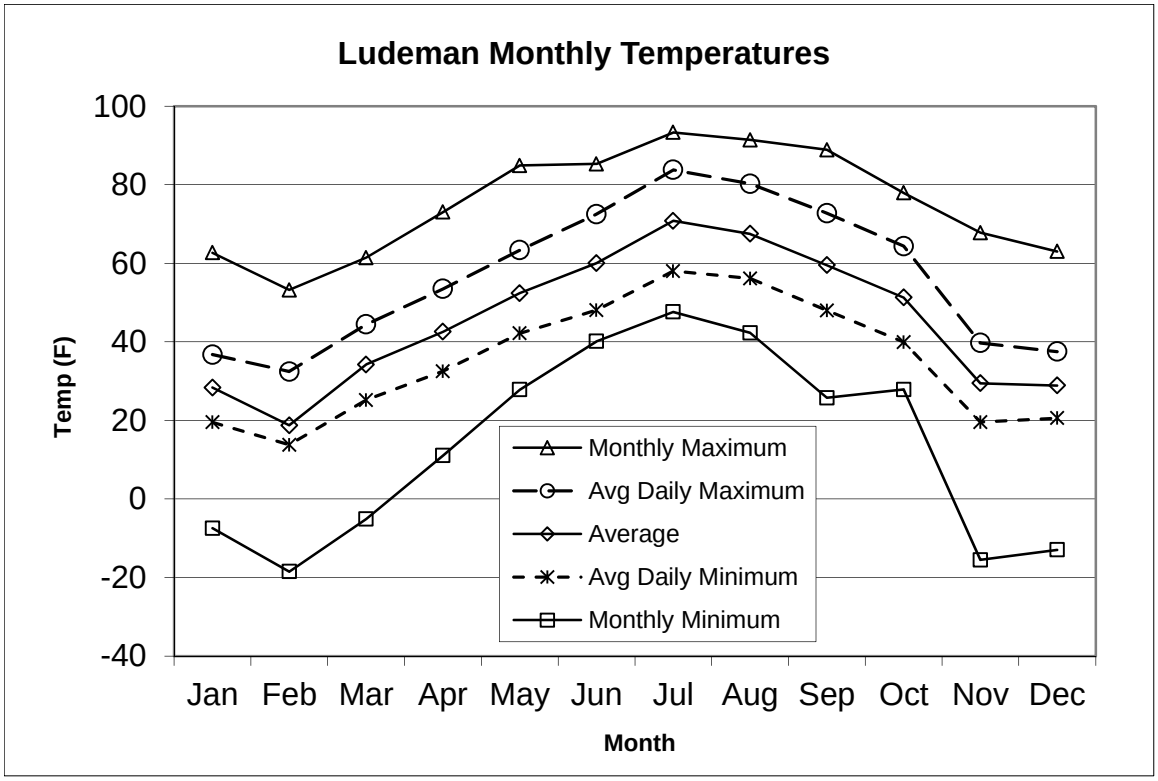

Figure 2 – Ludeman Diurnal Average Temperatures

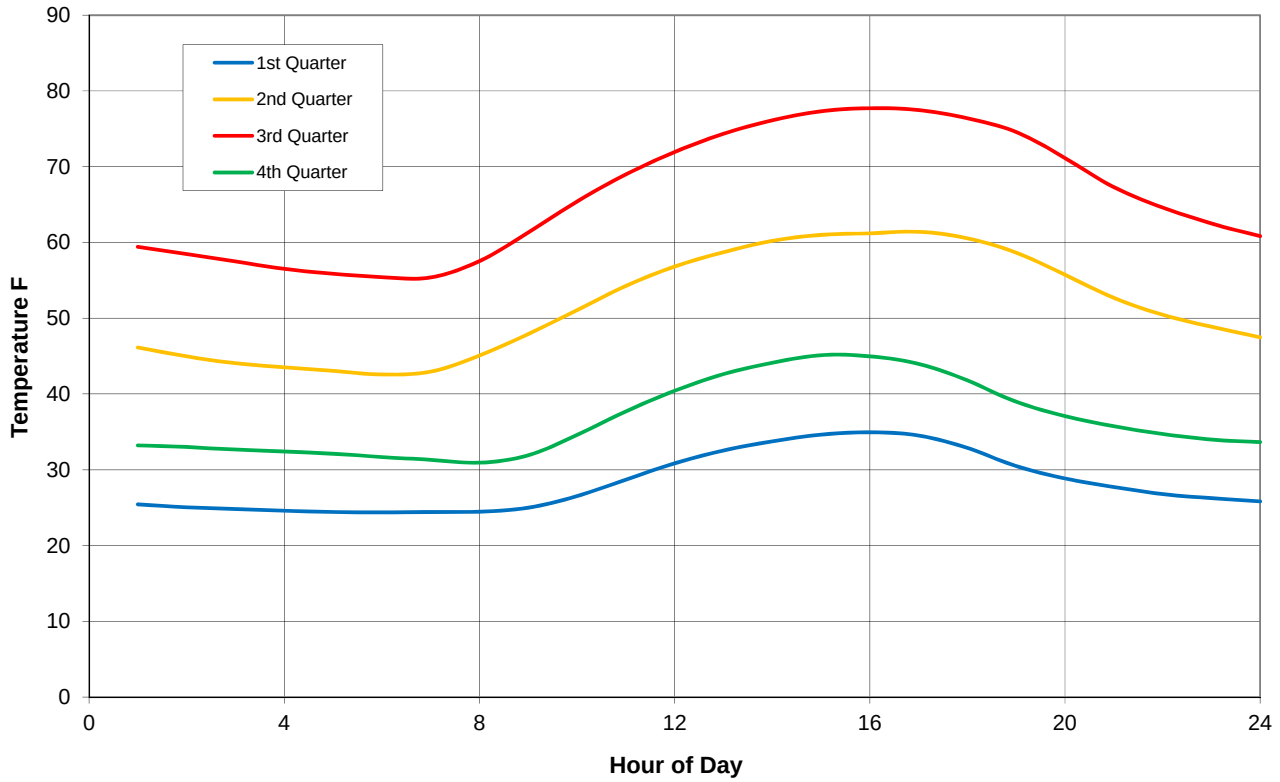

2.2 Wind Patterns

The baseline-year wind rose for the Ludeman site is presented in Figure 3, along with seasonal wind roses. Predominant winds are from the west and west-southwest, with spring and summer exhibiting a secondary east-southeasterly mode. Figure 4 shows the wind speed frequency and cumulative frequency distributions. The median wind speed is 11 mph and winds average over 18 mph 20% of the time. Figure 5 graphs monthly average wind speeds, which exceed 10 mph every month of the year. Also graphed in Figure 5 are peak hourly average wind speeds, which exceed 30 mph every month of the year. Diurnal average wind speeds, by calendar quarter, are shown in Figure 6. The strongest winds typically occur during afternoon hours.

Figure 3 – Ludeman Site Wind Roses

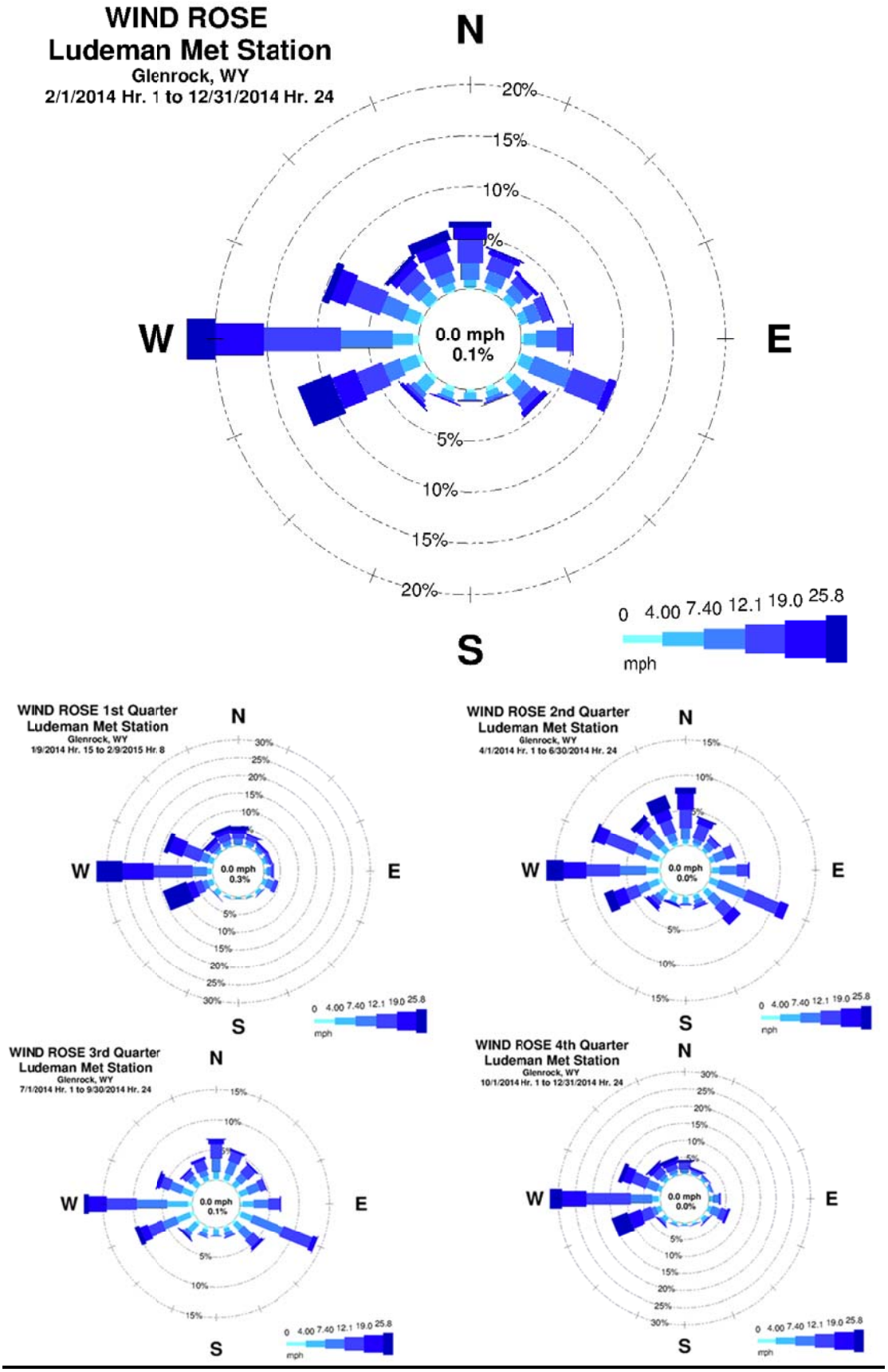

Figure 4 – Ludeman Site Wind Speed Frequency Distribution

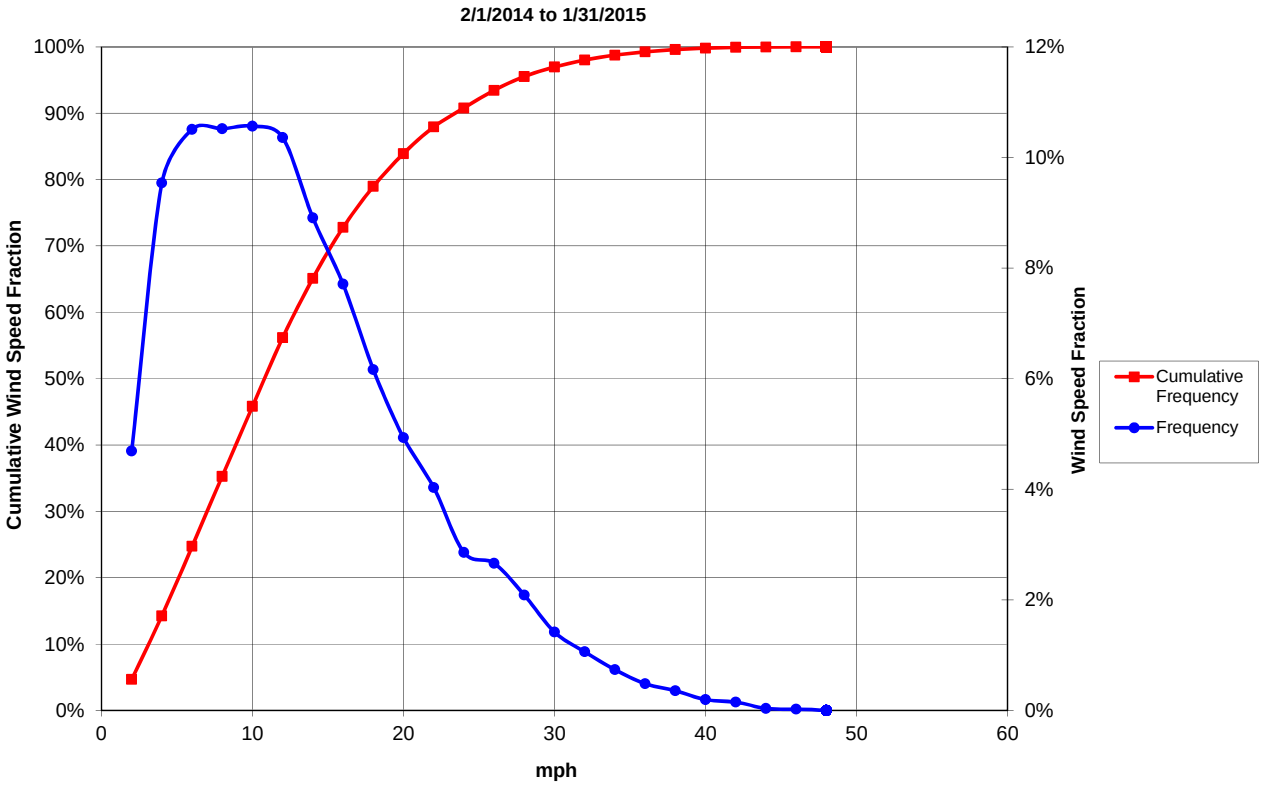

Figure 5 – Ludeman Site Monthly Wind Statistics

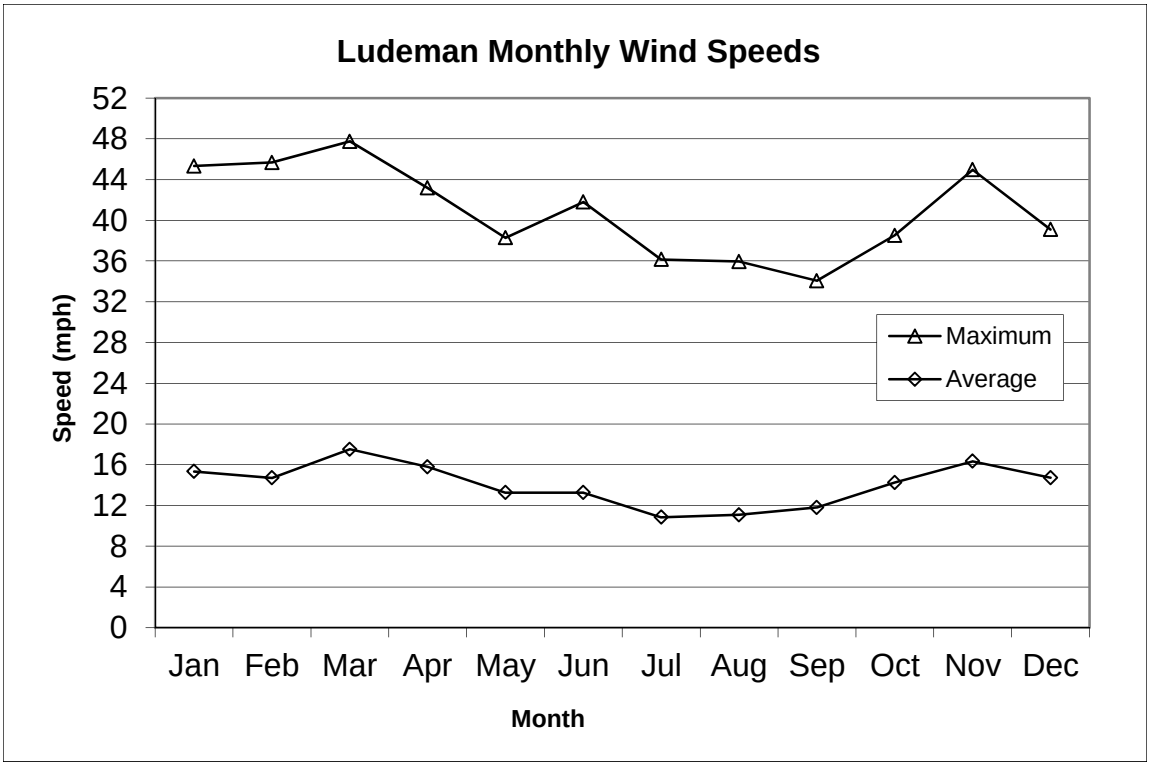

Figure 6 – Ludeman Diurnal Wind Speeds

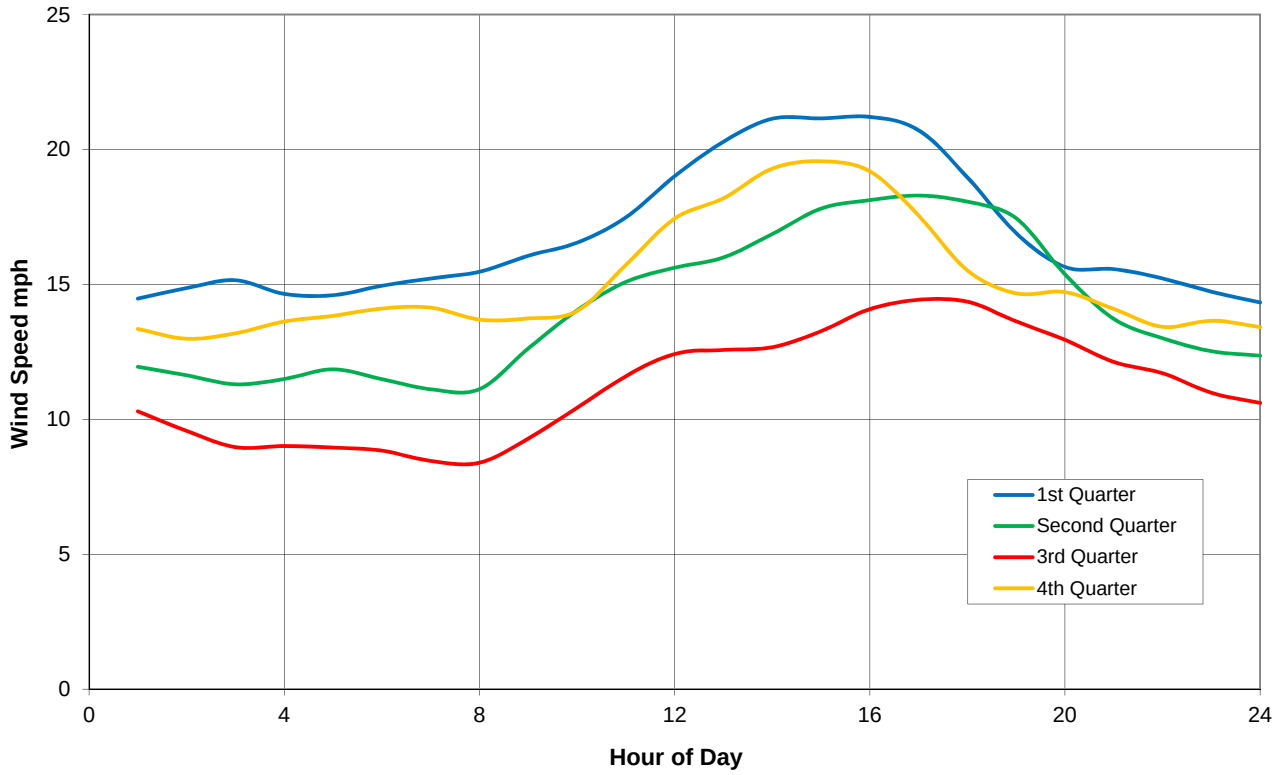

2.3 Precipitation

Monthly precipitation totals are shown in Figure 7. June was the wettest month, with December recording only 0.01 inches of precipitation. Total precipitation for the baseline year was 7.94 inches.

Figure 7 – Ludeman Site Monthly Precipitation

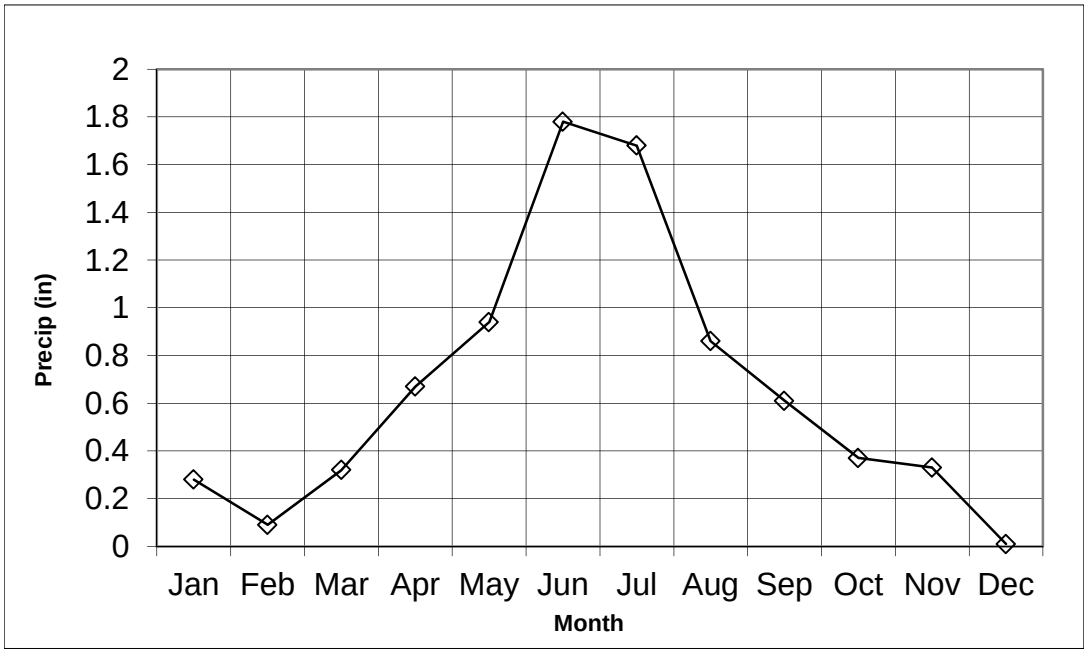

2.4 Relative Humidity

Figure 8 graphs monthly average relative humidity, as well as average daily high and low relativity (RH) by month. Average RH values range from 50% in July to nearly 75% in February. Daily high, hourly average RH peaks at 90% in May while daily lows reach a minimum of 30% in July. Figure 9 shows the diurnal variation. Both seasonal and diurnal variations are largely an artifact of ambient temperatures. Relative humidity is a temperature based calculation which shows the fraction of moisture present divided by the amount of moisture for saturated air at that temperature. The dew point is the temperature at which the existing moisture in the air would reach saturation, and below which moisture would begin to condense. Warm air will hold more moisture than cool air; thus, for a given mass of moisture in the atmosphere, relative humidity will increase as the air cools.

Figure 8 – Ludeman Site Monthly Relative Humidity Statistics

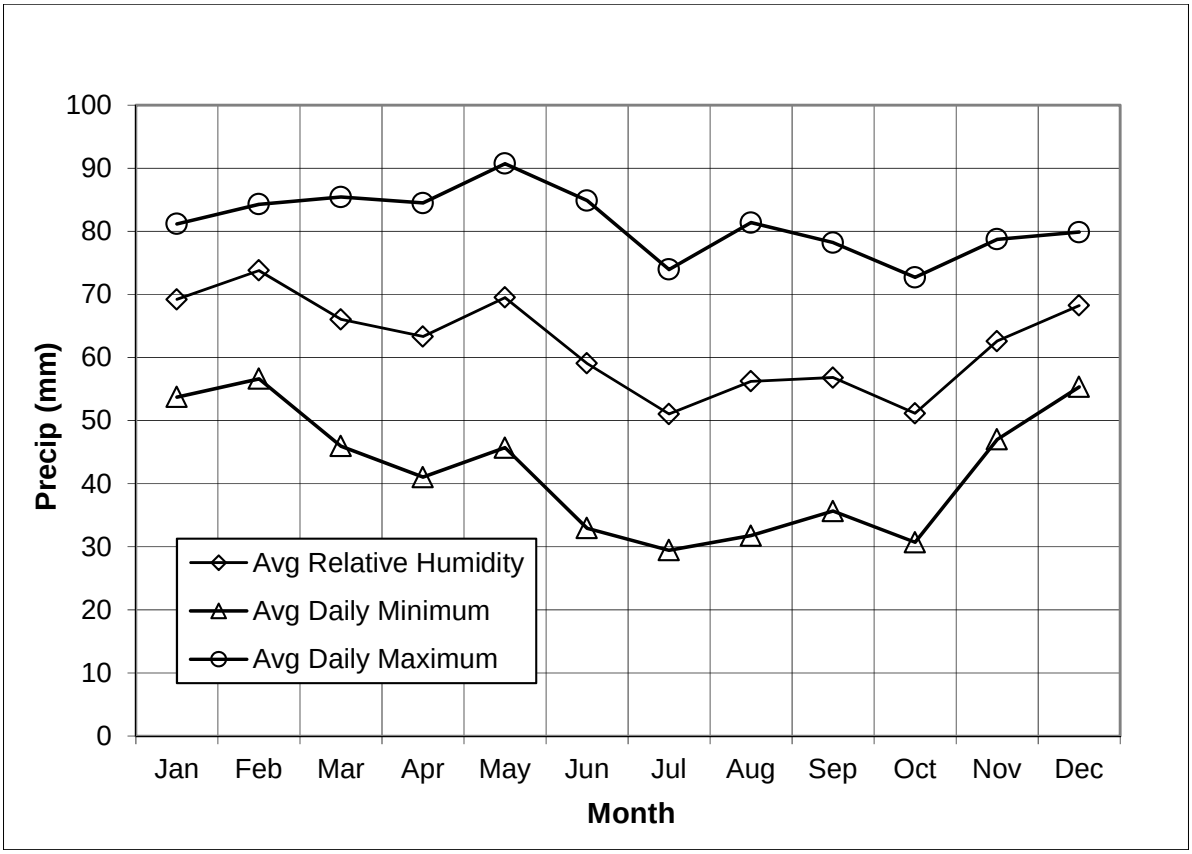

2.5 Solar Radiation and Evapotranspiration

Figure 10 graphs average solar radiation by month. Solar radiation values are used, along with wind speeds, daily high/low temperatures and daily high/low relative humidity to estimate monthy evapotranspiration using the Penman Equation. Figure 11 summarizes this calculation.

Figure 9 – Ludeman Site Diurnal Relative Humidity

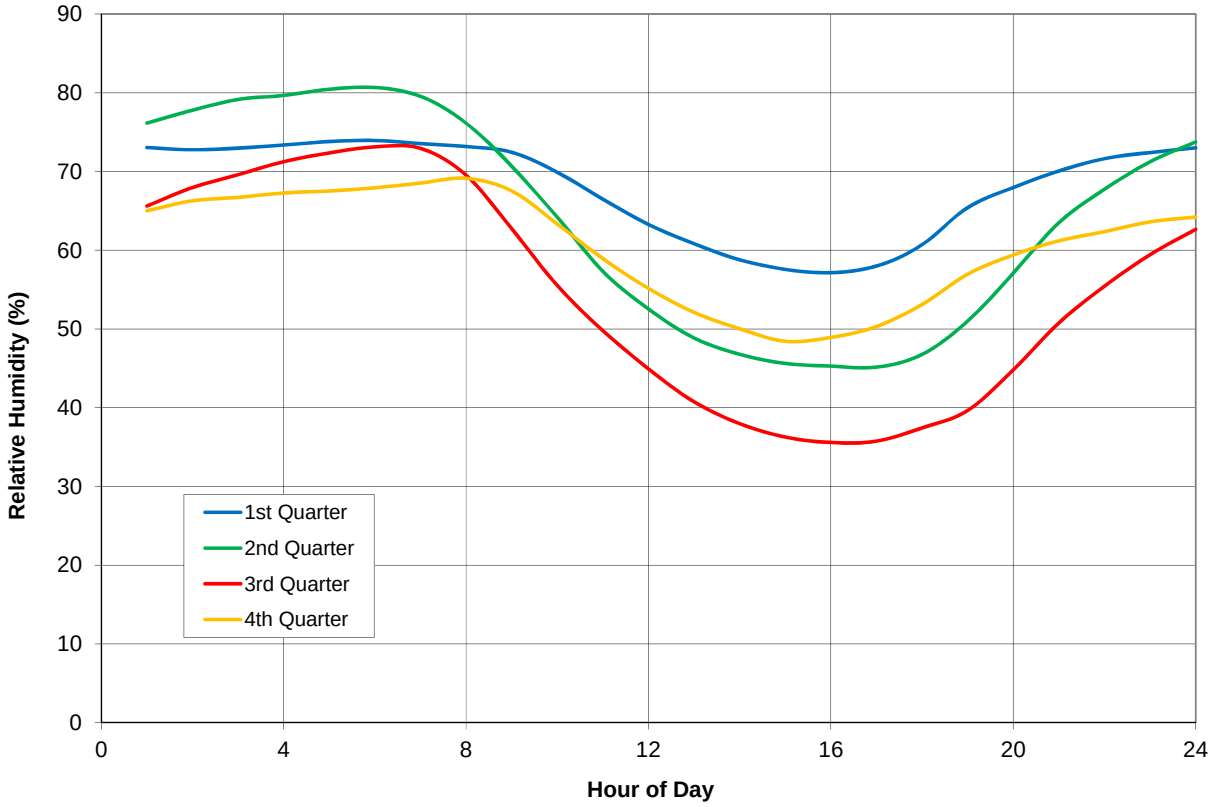

Figure 10 – Ludeman Site Monthly Average Solar Radiation

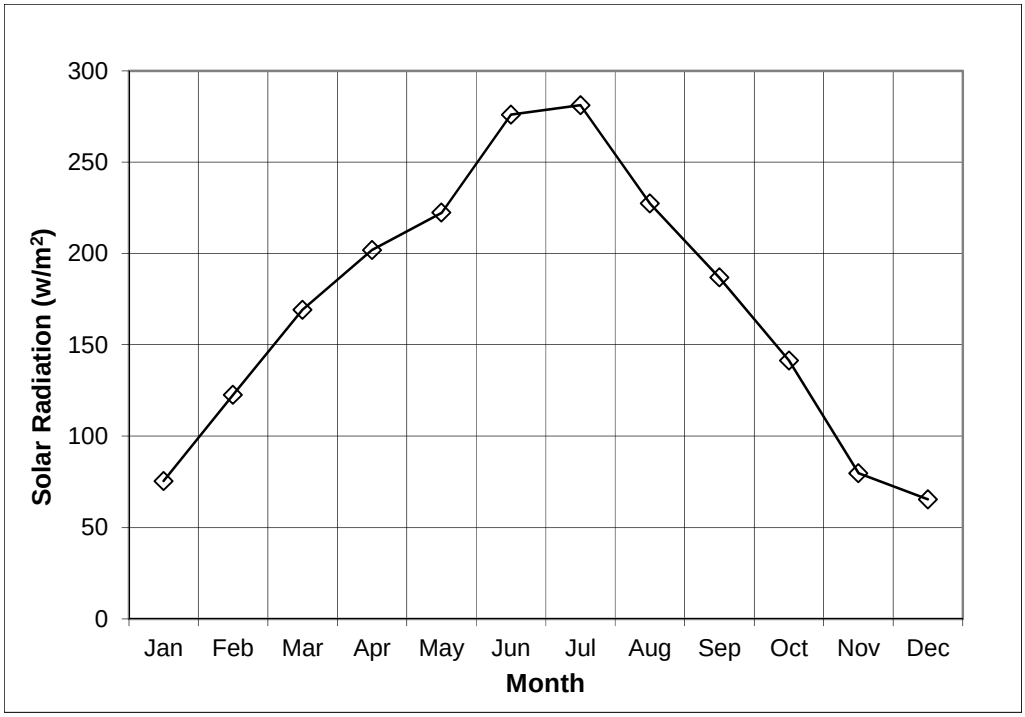

Figure 11 – Ludeman Site Monthly Evapotranspiration

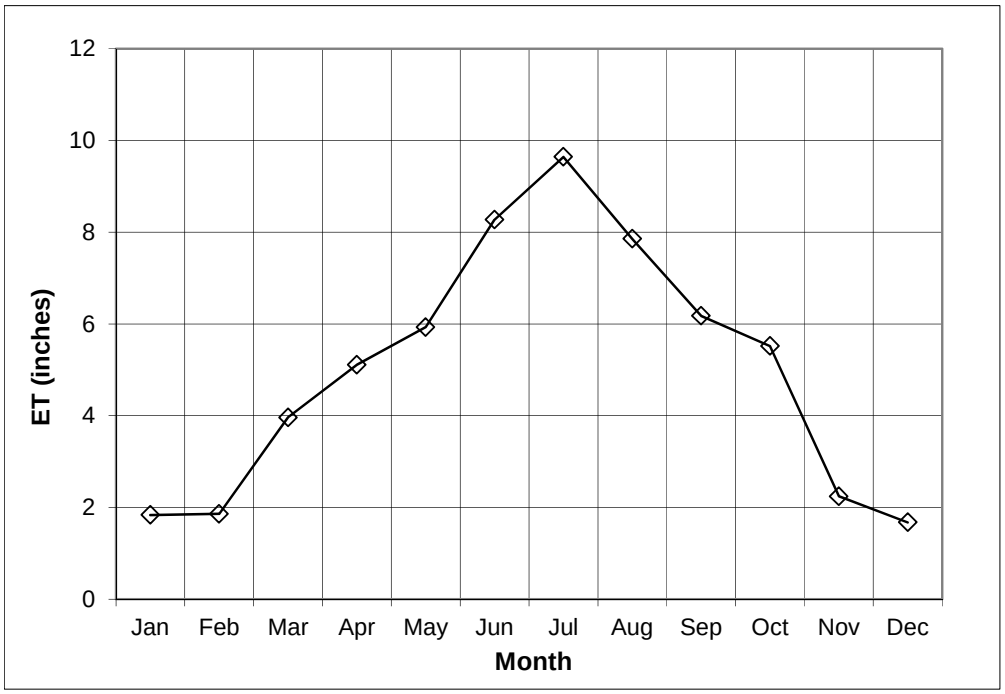

2.6 Atmospheric Stability

Atmospheric stability classes were assigned to each hour according to the σ_θ method (EPA 2000). Alternatively, these classes were also derived from solar radiation and temperature gradient (SRDT method). Figure 12 compares the stability class distributions from these two methods. Stabiity Class D, designated as neutral to slightly unstable conditions, dominates for both methods.

Figure 12 – Ludeman Atmospheric Stability Class Distribution

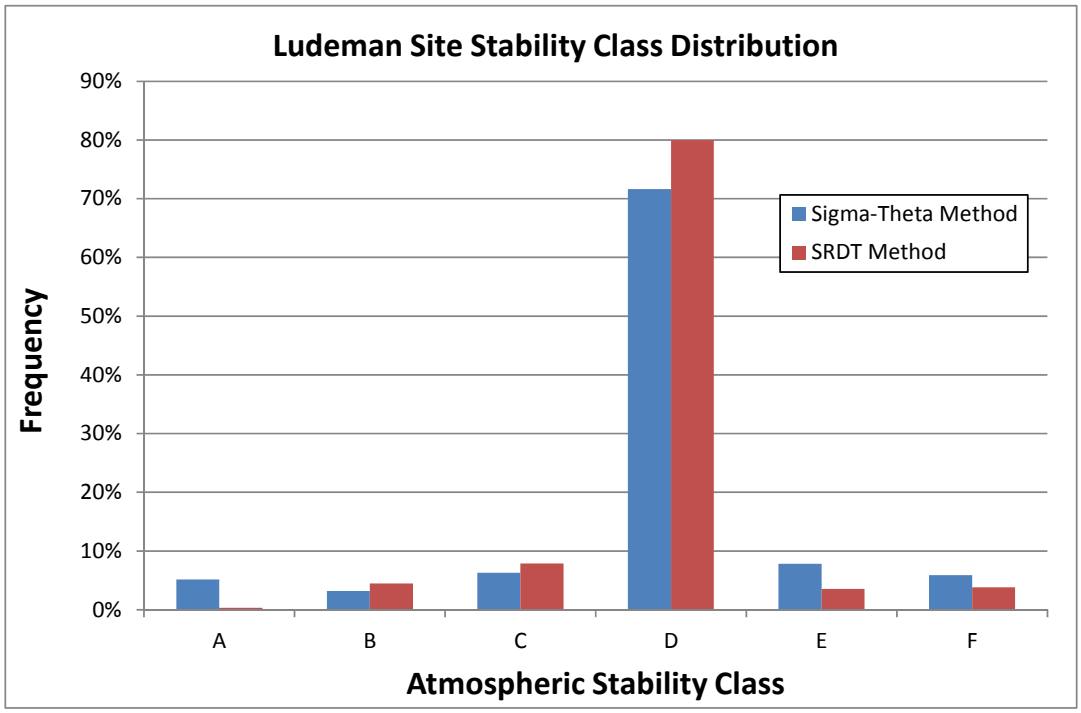

3.0 Comparison of On-Site Meteorology to Off-Site Data

In the original license application, the Ludeman site meteorology was approximated using hourly average data from the nearby Douglas Airport and Glenrock Coal Mine. NRC staff observed that while these surrogate sites are within 15 miles of the Ludeman Project area, significant topographic relief separates Ludeman from these other sites and potentially introduces differences in local meteorology. Baseline-year, on-site monitoring has confirmed these differences, particularly with respect to wind patterns.

Figure 13 shows that wind speed and direction distributions at Douglas were similar between the baseline monitoring year and the previous 11 years. Figure 14, however, shows significant differences between the Douglas wind rose and the Ludeman site wind rose.

Figure 13 – Douglas Long-Term and Baseline Year Wind Roses

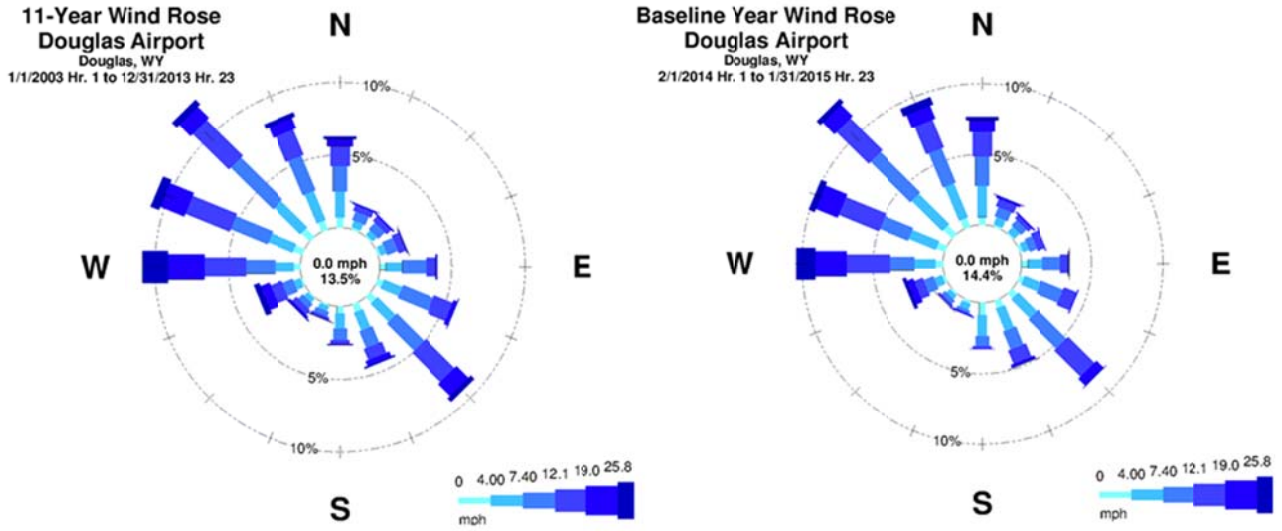

Figure 14 – Douglas vs. Ludeman Site Wind Roses

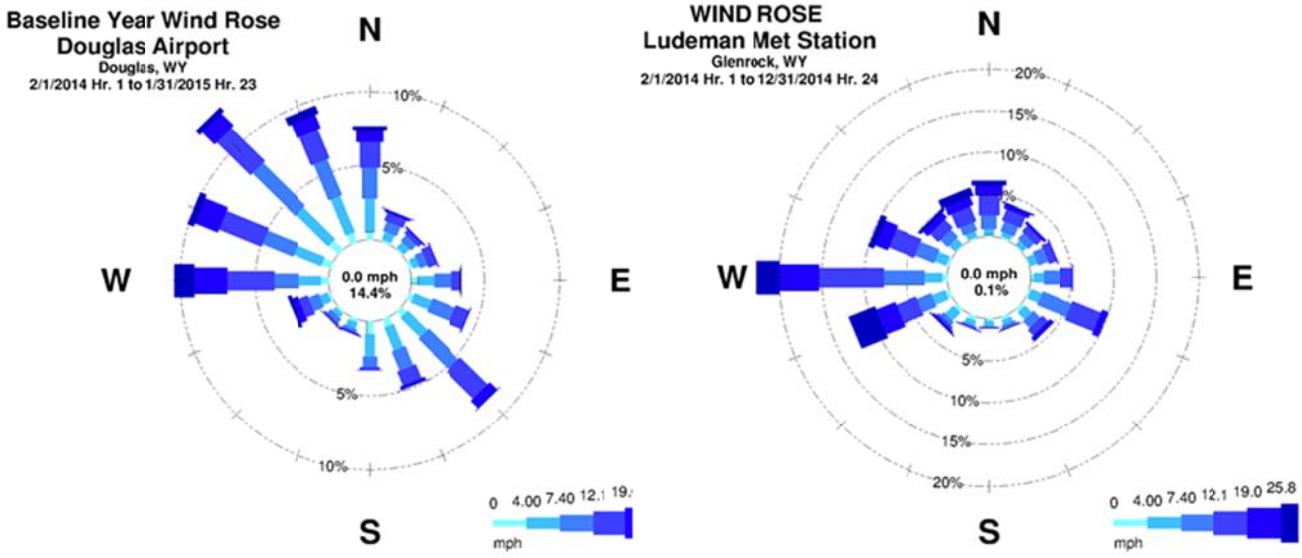

These differences may be attributed in part to the funneling of northwesterly winds and the shielding of southeasterly winds by the Laramie Mountains at the Ludeman site. The same mountains shield Douglas from the west-southwesterly winds prominent at Ludeman, but do not block or redirect winds emanating from the north to northwesterly directions.

Figure 15 compares the Glenrock long-term wind rose with the Ludeman on-site wind rose (note that Glenrock monitoring was discontinued in 2010). The Glenrock location exhibits greater similarity to the Ludeman site than Douglas, perhaps owing to its similar relationship to the mountains. Glenrock is slightly farther from the mountain range and higher than the Ludeman site.

Figure 15 – Glenrock vs. Ludeman Site Wind Roses

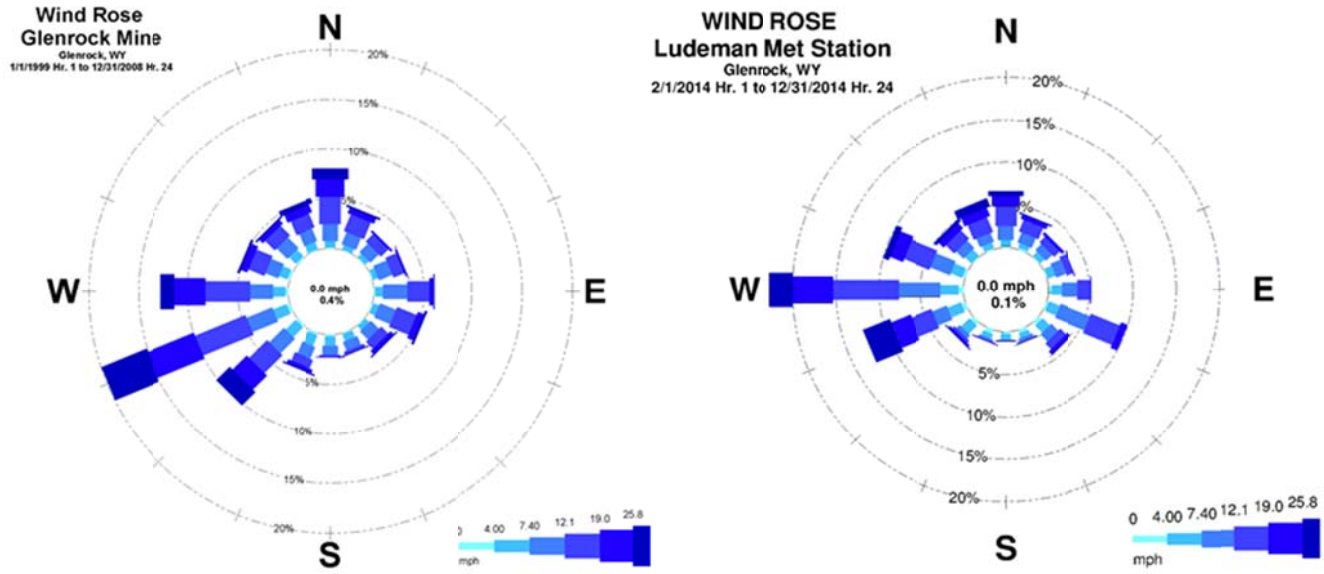

The regression lines in Figure 16 substantiate the dissimilarity between Douglas and Ludeman wind roses. The respective wind speed frequency distributions are only mildly related (R^2 = 0.55) and the wind direction frequency distributions are not related at all (R^2 = 0.03).

Figure 16 – Douglas vs. Ludeman Site Wind Frequency Correlations

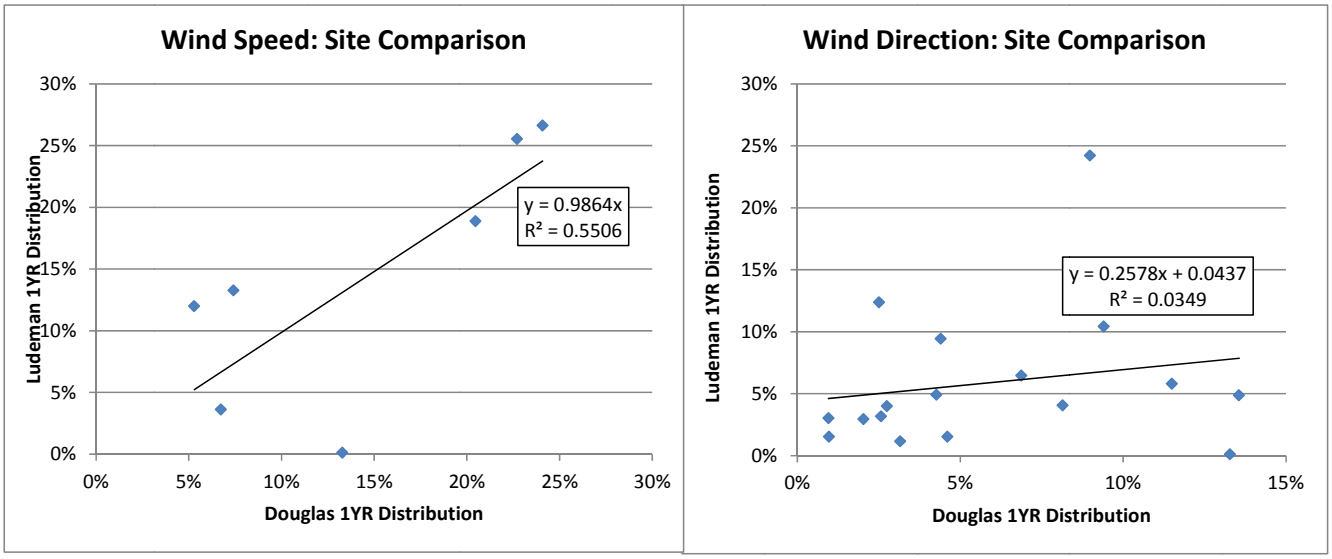

The regression lines in Figure 17 are consistent with the moderate agreement between Douglas and Ludeman wind roses. The respective wind speed frequency distributions are strongly related (R^2 = 0.97) and the wind direction frequency distributions are mildly related (R^2 = 0.48).

Figure 17 – Douglas vs. Ludeman Site Wind Frequency Correlations

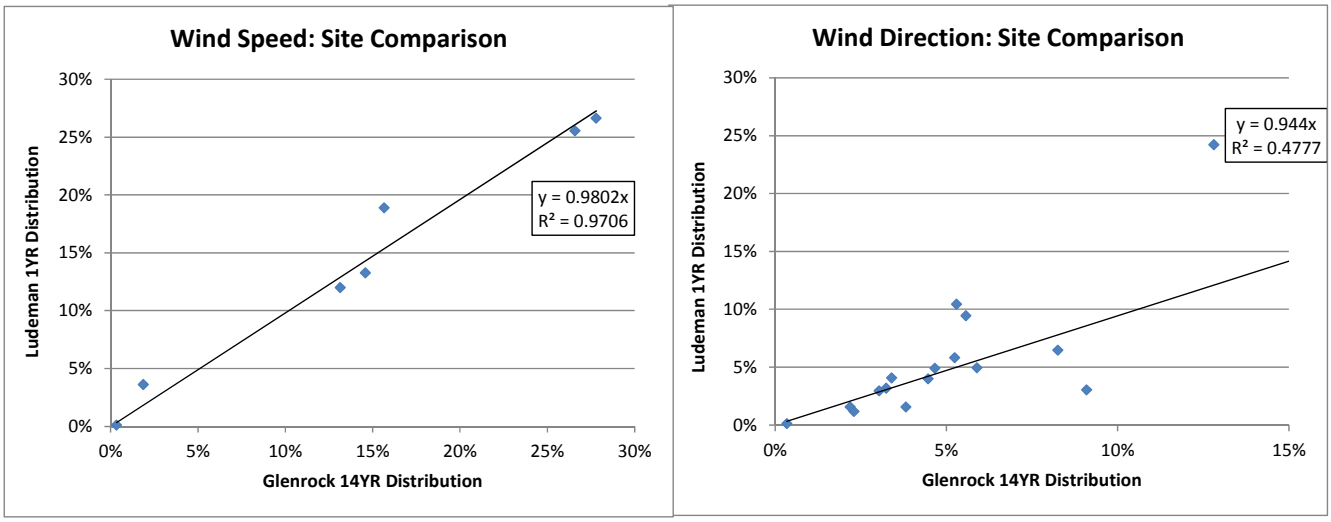

In conclusion, neither off-site wind data set closely matches the on-site data. This confirms the merits of the on-site meteorological monitoring program.

4.0 Long-Term Representativeness of Baseline Monitoring Year

In response to previous guidance from NRC, this report applies alternative statistical tests to the comparison of short and long-term, hourly wind speed and wind direction data at a representative site (Casper Airport). Appendix A of this report documents and evaluates these alternative tests for their appropriateness in comparing meteorological frequency distributions. The alternatives considered include summary statistics, the chi-square test, the Student's t-test, the Kolmogorov-Smirnov test, and linear correlation/regression analysis. Appendix A presents a case study based on three sites with available long-term meteorological data. This allows temporal comparisons for each site, as well as inter-site comparisons to assess how well each statistical test discriminates between visually similar and dissimilar frequency distributions.

4.1 Data Sources

U1 Americas has collected over one year of hourly meteorological data at its Ludeman ISR Project site (IML 2015a). For the purposes of MILDOS modeling and this analysis, the first year serves as the baseline period. For comparing long-term meteorological conditions to short-term conditions, hourly data from the Casper Airport (NCDC 2015) were used. Casper was selected due to several factors:

1. Operated by the National Weather Service, meeting NRC guidance in Regulatory Guide 3.63
2. Proximity to the Ludeman Project site (40 miles to the west), similar elevation, terrain and relationship to east-west trending mountain range to the south
3. Longest period of record within a 50-mile radius, with 18 years of hourly data available in electronic form

The short-term period is synchronous with the baseline monitoring year at the Ludeman site, from February 1, 2014 through January 31, 2015. The long-term period is defined as 1997 through 2013, or 17 calendar years. Thus, there is no overlap between short-term and long-term data sets. Hourly wind speed and wind direction data are categorized to form short and long-term frequency distributions. Wind speeds are divided into 6 classes (plus a 7^{th} calm class), and wind directions are divided into 16 classes (plus a 17^{th} calm class). These classification schemes correspond directly to the MILDOS STAR distribution. Appropriate statistical tests from the list enumerated above, are employed to determine if there is a significant difference between the short and long-term distributions of classified Casper data.

Notwithstanding the example of 30 years cited in NRC Regulatory Guide 3.63, 17 years are deemed adequate to represent long-term meteorological data. Appendix A to this report documents this and cites the risks of using too long a period of record (POR). In particular, a publication from the U.S. Air Force Climatology Center (Coffin 1996) states, "As the POR expands, maintaining homogeneity of the data becomes more difficult. Climatological statistics obtained from too long a period may not be representative of contemporary conditions."

4.2 Graphical Methods

Histograms, scatterplots and wind roses provide a visual demonstration of the similarities between short and long-term meteorological data at Casper. Figure 18 compares the 1-year (baseline) and 17-year wind frequency distributions. It can be seen that both wind speed and wind direction frequencies are distributed similarly over the two time periods.

Figure 18 – Casper Long-Term and Short-Term Wind Frequency Distributions

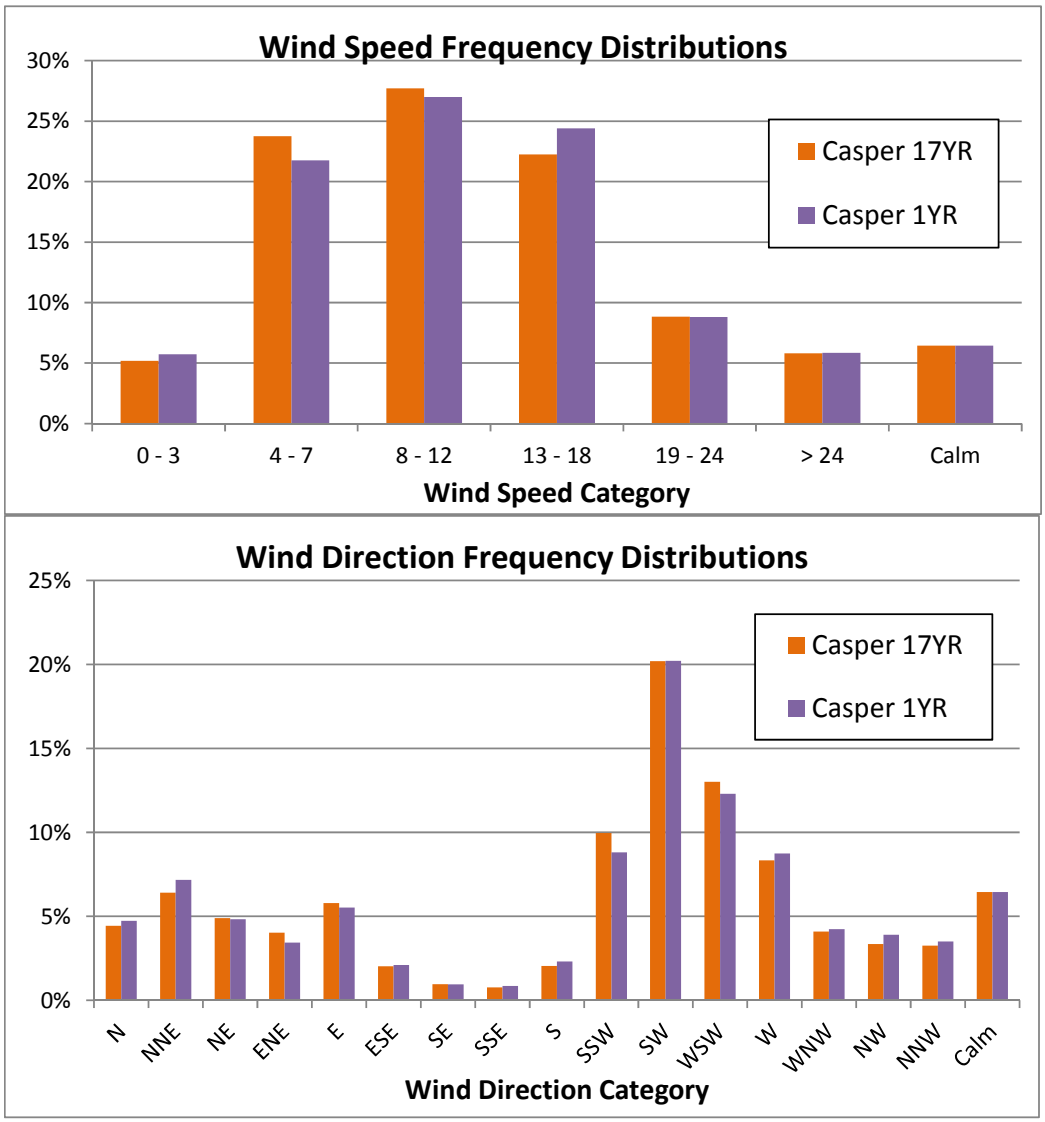

Figure 19 shows the wind roses from Casper for the same periods. The wind rose provides a polar graph of the joint distribution of wind speed and wind direction frequencies.

Figure 19 – Casper Long-Term and Short-Term Wind Roses

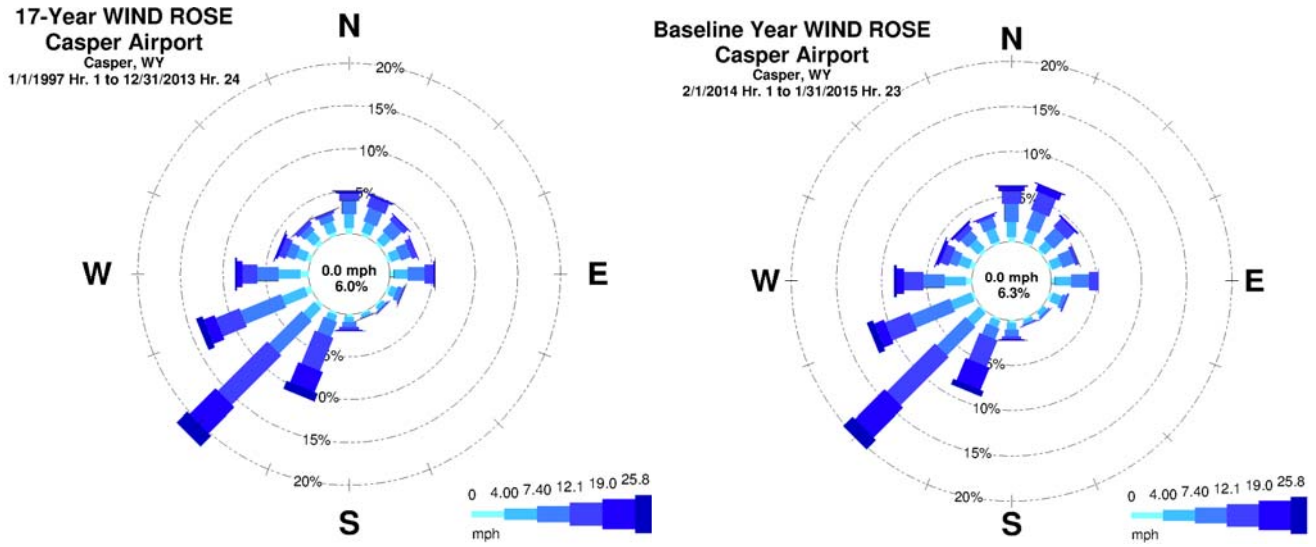

Figure 20 graphs the short-term vs. long-term wind frequencies, demonstrating close correlation between the two wind speed distributions and between the two wind direction distributions. In this instance, the right-most point on the wind speed graph corresponds to the 8-12 mph category, which accounts for 27% of the hourly wind speeds for the baseline year (y-axis), and 28% of the hourly wind speeds over the previous 17 years (x-axis). The other points correspond to the remaining 6 wind speed categories. The wind direction graph plots the 17 direction categories in similar fashion.

Figure 20 – Casper Long-Term and Short-Term Wind Speed and Direction Scatterplots

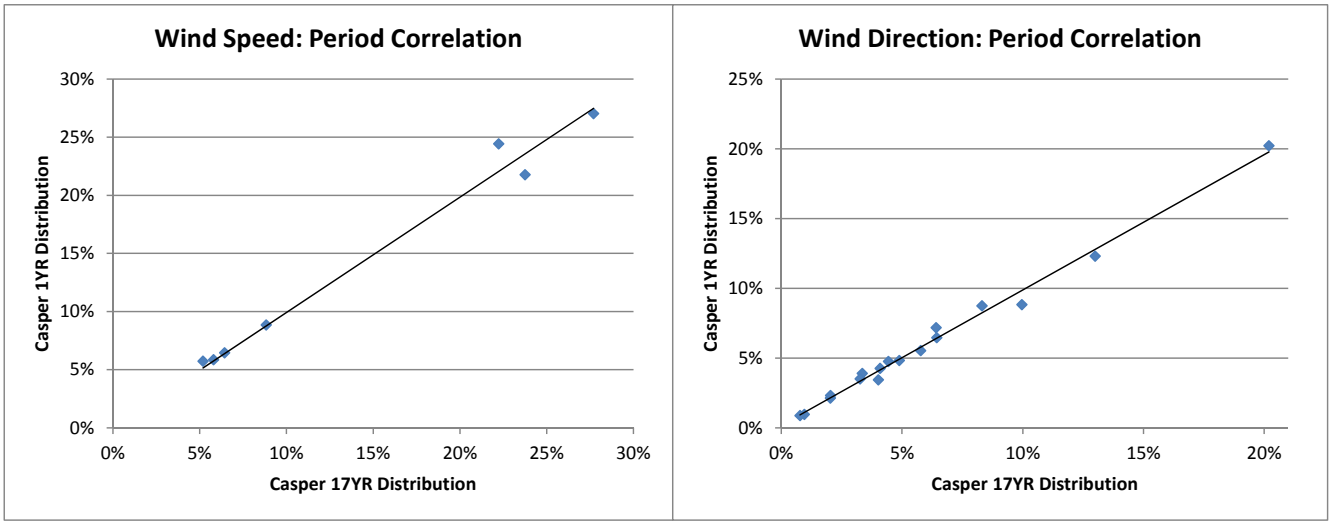

Figure 21 graphs the short-term vs. long-term joint wind speed and direction frequencies, once again demonstrating close correlation between the two periods for each of the 97 joint categories. Figure 21 substantiates the similarity between wind roses in Figure 19.

Figure 21 – Casper Long-Term and Short-Term Joint Wind Speed and Direction Scatterplot

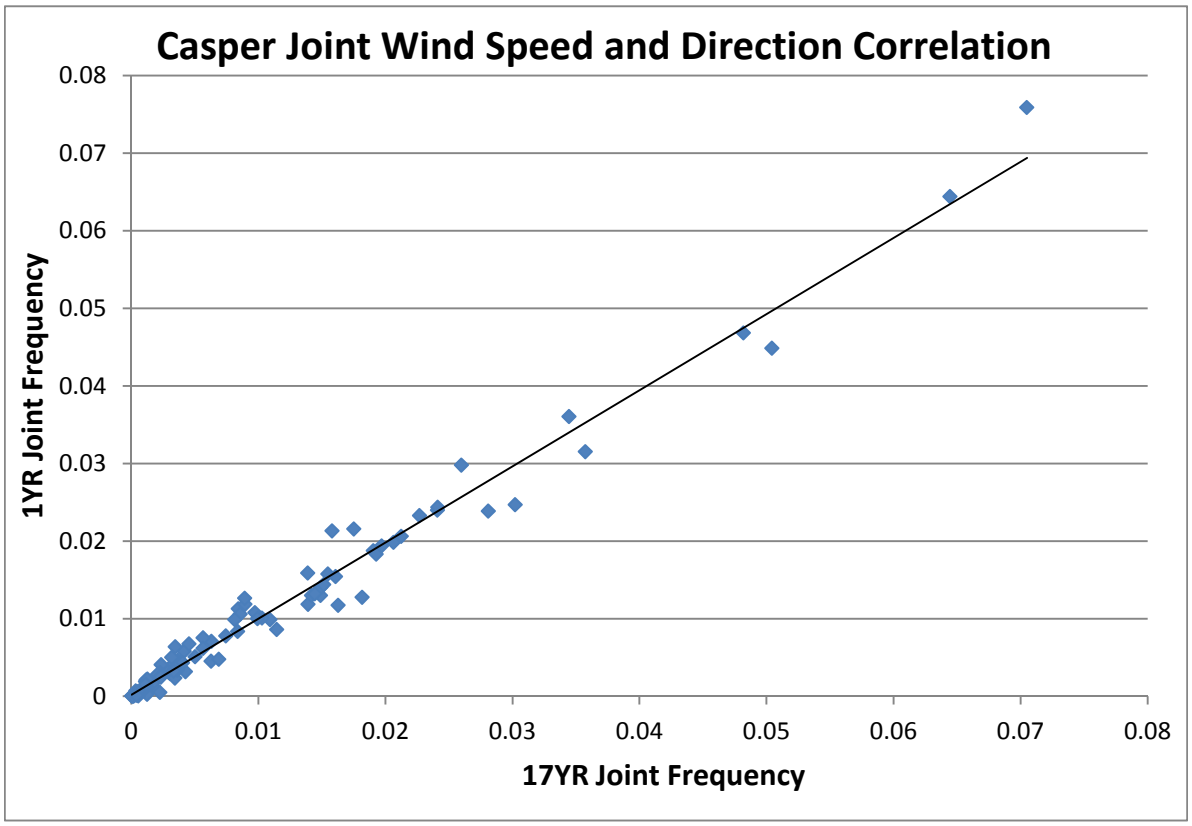

4.3 Summary Statistics

Table 1 shows the average wind speed, unit-vector averaged wind direction, and vector averaged wind direction for the 17-year monitoring period and for the 1-year baseline period. Between the two periods, these statistics are quite similar.

Table 1 – Casper Wind Speed and Direction Summary Statistics

Statistic	Average Wind Speed (mph)	Unit Vector Average Wind Direction (°)	Wind Speed Vector Average Wind Direction (°)
1997 through 2013	10.9	249.4	239.4
Baseline Year	11.2	254.0	244.5

4.4 Application of the Chi-Square (χ^2) Test

The χ^2 test can be used to evaluate the null hypothesis (H_0) that two frequency distributions are similar. Appendix A demonstrates some limitations in the χ^2 test when applied to frequency distributions derived from large samples. It discusses the usefulness of converting relative frequencies to equivalent annual hours, then adjusting the χ^2 value for large sample size by means of the phi coefficient.

In this analysis, the χ^2 test regards long-term values as the expected hourly counts per year, and short-term (baseline period) values as the observed counts per year. Table 2 shows the resulting analysis of wind speeds at Casper. The calculated χ^2 value of 39.70 is more than the 95% confidence statistic for 6 degrees of freedom (12.59). Thus, for this sample size (8,760) we reject H_0, which states that the short-term wind speed distribution comes from the same population as (i.e., is representative of) the long-term distribution. However, due to the liabilities of the Chi-Square test in treating large samples, we compute the phi coefficient, which adjusts the χ^2 result for large sample sizes, as 0.07. This infers similarity between the two wind speed distributions. An analysis of categorized cloud cover by the U.S. Air Force established a critical phi coefficient of 0.20, below which "a large degree of similarity" between distributions is indicated (Lowther 1991). Note that the minimum annual count of 455 (0 - 3 mph) is larger than the minimum recommended by NRC (NRC 2011) for a valid χ^2 test.

Table 2 – χ^2 Test for Annualized Wind Speed Distributions

Wind Speeds - Casper LT/ST Frequency x 8,760				
mph	17Yr WS	1Yr WS	$(LT-ST)^2/LT$	Chi-Square
0 - 3	455	501	4.691	39.70
4 - 7	2082	1905	14.908	$\chi^2_{0.95}(6) = 12.59$
8 - 12	2427	2366	1.548	**Reject H_0**
13 - 18	1949	2139	18.541	p-value = 0.000
19 - 24	774	773	0.002	Min Count = 455
> 24	509	511	0.015	Phi-value = 0.07
Calm	564	564	0.000	**Adj: Do Not Reject**

Table 3 shows a similar test for 17-year vs. 1-year wind directions at Casper. The calculated χ^2 value of 48.96 is more than the 95% confidence statistic for 16 degrees of freedom (26.30), so we initially reject the null hypothesis (H_0) that the short-term wind direction distribution comes from the same population as the long-term distribution. The phi coefficient of 0.07, however, suggests a strong similarity between the two wind direction distributions. As with wind speeds, the minimum annual count of 68 (SSE) is sufficient for a valid χ^2 test.

If the wind direction frequencies are multiplied by 1,000 rather than by 8,760, the χ^2 test in Table 4 produces a different outcome (Table 5). In this case the calculated χ^2 value of 5.59 is less than the critical value, so we cannot reject H_0 with 95% confidence. As pointed out in Appendix A, the χ^2 test is sensitive to large sample sizes. The phi coefficient removes this sensitivity. Though the χ^2 statistics are different, a sample size of 1,000 (Table 4) and a sample size of 8,760 (Table 3) both yield the same phi coefficient of 0.07. Neither version of the test ultimately provides sufficient evidence to reject H_0.

Table 3 – χ^2 Test for Annual Wind Direction Distributions

Wind Directions - Casper LT/ST Frequency x 8,760				
Direction	17Yr WD	1Yr WD	$(LT-ST)^2/LT$	Chi-Square
N	389	415	1.755	48.96
NNE	562	628	7.800	$\chi^2_{0.95}(16) = 26.30$
NE	428	422	0.086	**Reject H_o**
ENE	353	300	7.780	p-value = 0.000
E	506	483	1.053	Min Count = 68
ESE	178	185	0.224	Phi-value = 0.07
SE	84	83	0.001	**Adj: Do Not Reject**
SSE	68	75	0.777	
S	179	202	3.038	
SSW	873	772	11.720	
SW	1770	1770	0.000	
WSW	1139	1076	3.471	
W	729	765	1.791	
WNW	358	371	0.461	
NW	294	341	7.549	
NNW	286	306	1.458	
Calm	564	564	0.000	

Table 4 – χ^2 Test for Wind Direction with Smaller Scaling Factor

Wind Directions - Casper LT/ST Frequency x 1000				
Direction	17Yr WD	1Yr WD	$(LT-ST)^2/LT$	Chi-Square
N	44	47	0.200	5.59
NNE	64	72	0.890	$\chi^2_{0.95}(16) = 26.30$
NE	49	48	0.010	**Can't reject H_o**
ENE	40	34	0.888	p-value = 0.992
E	58	55	0.120	Min Count = 8
ESE	20	21	0.026	Phi-value = 0.07
SE	10	9	0.000	**Adj: Confirm**
SSE	8	9	0.089	
S	20	23	0.347	
SSW	100	88	1.338	
SW	202	202	0.000	
WSW	130	123	0.396	
W	83	87	0.204	
WNW	41	42	0.053	
NW	34	39	0.862	
NNW	33	35	0.166	
Calm	64	64	0.000	

Table 5 shows the χ^2 test for wind speed frequencies multiplied by 1,000 instead of 8,760. The χ^2 statistic of 4.53 indicates non-rejection of H_0. The phi coefficient of 0.07 confirms this and is independent of the choice of sample size, again offering a more reliable measure of similarity.

Table 5 – χ^2 Test for Wind Speed with Smaller Scaling Factor

Wind Speeds - Casper LT/ST Frequency x 1000				
mph	17Yr WS	1Yr WS	$(LT-ST)^2/LT$	Chi-Square
0 - 3	52	57	0.535	4.53
4 - 7	238	218	1.702	$\chi^2_{0.95}(6) = 12.59$
8 - 12	277	270	0.177	**Can't reject H_o**
13 - 18	222	244	2.117	p-value = 0.605
19 - 24	88	88	0.000	Min Count = 52
> 24	58	58	0.002	Phi-value = 0.07
Calm	64	64	0.000	**Adj: Confirm**

The χ^2 test results above indicate insufficient evidence to infer a statistical difference between short and long-term wind speed and wind direction distributions. This is not always the case. Appendix A illustrates that even when corrected for large samples, the χ^2 test generally infers a significant difference between wind frequency distributions from different sites.

4.5 Evaluation of the Student's T-Test

The two-sample t-test can be used to assess similarity between two frequency distributions, if those distributions are expanded to form year-to-year frequencies within each individual data category. Appendix A eliminates two-sample t-tests conducted in the manner of the χ^2 test discussed above. Such a test evaluates differences between two complete frequency distributions, but in this application the short and long-term frequencies will always have the same mean (1/C, where each of the paired distributions has C categories). Under these circumstances the t-test will always show equivalence.

Alternatively, the two-sample t-test can be applied separately to each wind speed and wind direction category. This scenario is only effective when comparing two multi-year distributions, since both short-term and long-term variability are needed. Therefore, this approach is not practical for the single-year baseline monitoring period at the Ludeman site.

4.6 Evaluation of the Kolmogorov-Smirnov Test

The Kolmogorov-Smirnov (K-S) test is a nonparametric test for the equality of continuous, one-dimensional probability distributions that can be used to compare two samples without many of the assumptions required for other statistical methods. In exchange for this broad applicability, the K-S test sacrifices statistical efficiency. The case study in Appendix A shows that all inter-site comparisons using the K-S test result in the false conclusion that the wind speed and wind direction distributions are statistically no different. The respective wind roses, the χ^2 test, and linear regression analysis all contradict this result. While its consistent finding of insignificant differences superficially supports the case for representativeness, the inability of the K-S test to distinguish between clearly dissimilar wind patterns eliminates this method as an appropriate alternative.

4.7 Application of Linear Correlation and Linear Regression

The following discussion combines linear correlation and regression since they yield closely related statistics. Linear regression is used to compare wind speed and wind direction frequency distributions for several reasons:

1. To make the correlation visible (shows line of least-squares fit).
2. To isolate the percentage of inter-category variance that is predictable (R^2) from the percentage that is random ($1 - R^2$), an important measure of how well one frequency distribution represents another.
3. To enable a zero intercept, providing a slightly more conservative R^2. A non-zero intercept implies a systematic bias, which is technically not possible between two frequency distributions that each sum to one.

Linear regression, without a forced zero intercept, produces a coefficient of determination R^2 which is precisely the square of the Pearson coefficient R generated by linear correlation. With the forced zero intercept this relationship is only approximate, but always errs on the side of conservatism (i.e., the square root of the coefficient of determination is always less than or equal to the correlation coefficient). While linear regression has not been commonly employed to demonstrate the degree of similarity between two meteorological frequency distributions, linear correlation coefficients have (Coffin 1996). Appendix A offers an in-depth analysis of linear correlation and regression in the context of meteorological frequency distributions.

A correlation coefficient is merely a mathematical expression of the “correspondence” between two distributions (Brooks 1978). In the present application, the short and long-term data distributions both approximate a third variable, the true long-term distribution. If any two relative frequency distributions of a categorized meteorological parameter are linearly correlated, they are also substantially equivalent since the frequencies sum to 1 for both distributions. And if they are equivalent, then either they both represent the true long term distribution, or neither does.

Figure 22 illustrates the linear association between short and long-term wind speed frequencies at Casper. In keeping with convention, the less certain variable (short-term frequency) is assigned to the vertical (dependent) axis and the better-supported, long-term frequency is assigned to the horizontal (independent) axis. The hourly data for each distribution fall into one of 7 categories. The graph illustrates the degree to which the 1-year frequencies match the 17-year frequencies. The R^2 value of 0.983 confirms a very strong linear relationship, and the slope of 0.992 indicates substantial equivalence between short and long-term frequencies. A p-value of zero establishes a near-100% confidence level that this relationship is significant.

Figure 23 illustrates the linear association between short and long-term wind direction frequencies at Casper, with the same choice of dependent and independent variables. The hourly data for each distribution fall into one of 17 categories. The graph illustrates the degree to which the 1-year frequencies match the 17-year frequencies. The R^2 value of 0.991 confirms a strong linear relationship, and the slope of 0.988 indicates substantial equivalence between short and long-term frequencies. A p-value of zero leaves little doubt that this relationship is significant.

Figure 22 – Casper Short and Long-Term Wind Speed Frequency Distributions

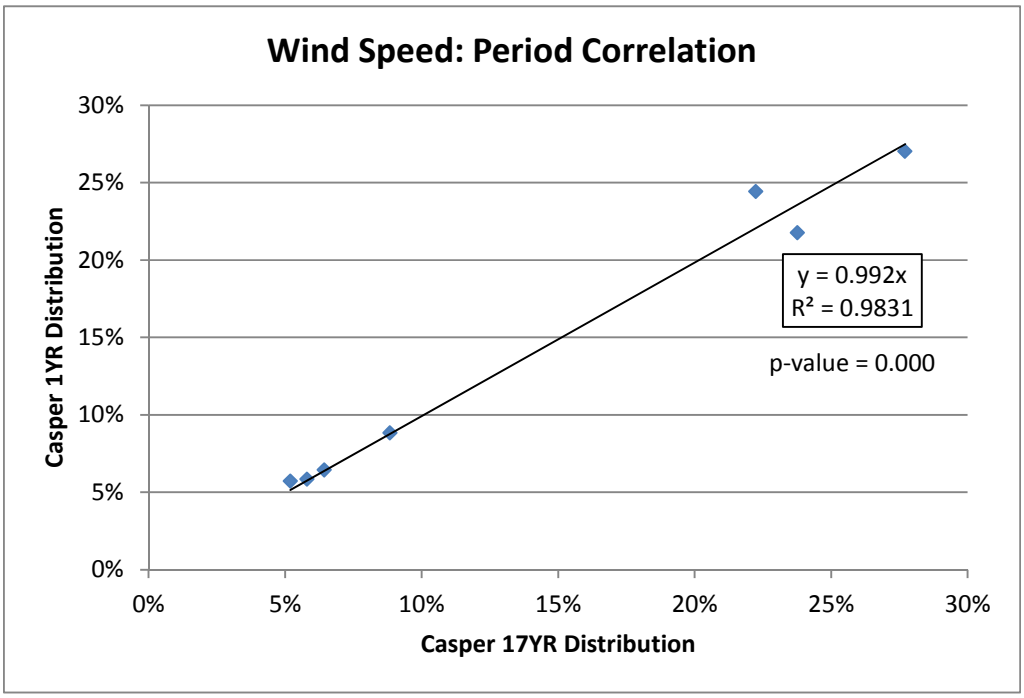

Figure 23 – Casper Short and Long-Term Wind Direction Frequency Distributions

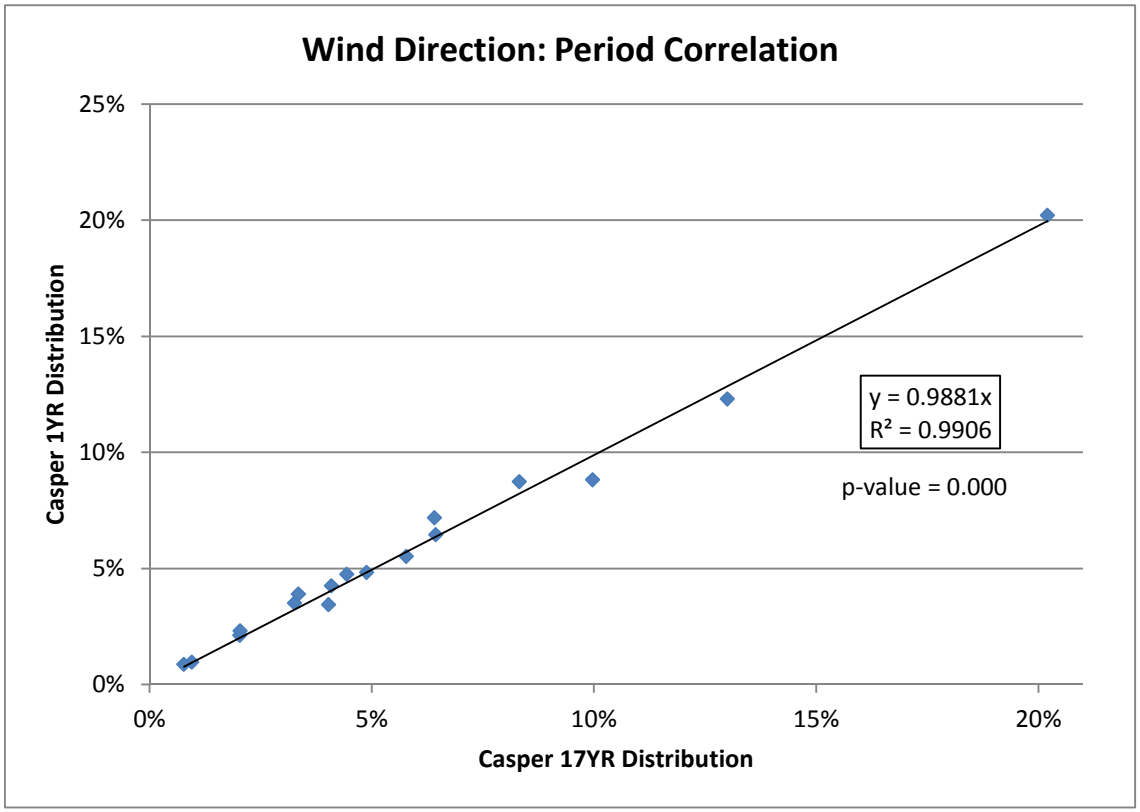

The MILDOS model accepts meteorological inputs in the form of joint wind speed, wind direction and stability class frequency distributions, also known as STAR distributions. An important subset of the STAR distribution is the two-way wind classification, which categorizes hourly wind data by both speed and direction. Hypothesis testing is generally unworkable in comparing joint wind speed and direction frequencies because the wind data are partitioned into too many categories. In general, the number of categories in hypothesis testing should not exceed $5*\log_{10}(N)$, where N is the sample size (Brooks 1978). For a one-year sample of hourly averages (N = 8,760) the maximum number of categories would be 20. This limit is consistent with 7 wind speed classes or 17 wind directions, but not with 97 joint frequency categories. Therefore the χ^2 test is not appropriate for evaluating similarities between joint frequency distributions.

Joint wind speed and direction distributions are amenable to linear regression or correlation. Analyzing these two-way distributions can strengthen the case for long-term representativeness of baseline wind data. The joint analysis offers a more rigorous comparison between short and long-term wind frequency distributions, than individual speed and direction analyses. This comparison also offers the best quantitative measure of the similarity between the associated wind roses (see Figure 19 and Figure 21).

Figure 24 shows the linear relationship between short and long-term joint frequencies at Casper. The hourly data for each distribution fall into one of 97 categories. The graph illustrates the degree to which the 1-year joint frequencies match the 17-year frequencies. The R^2 value of 0.979 confirms a very strong linear relationship, and the slope of 0.988 indicates substantial equivalence between short and long-term frequencies. A p-value of zero leaves little doubt that this relationship is significant.

Figure 25 graphs a short-term joint frequency distribution against the longer-term joint frequency distribution from the Douglas Airport, with similar results. Douglas also exhibits strong temporal correlation of joint wind frequencies. Figure 26 graphs the long-term joint frequency distribution from Douglas against that from Casper. The R^2 value of 0.108 indicates virtually no similarity between the two sites. The contrast to Figures 23 and 24 illustrates how effectively linear regression discriminates between similar and dissimilar wind regimes.

Linear regression also isolates the sources of variation among category frequencies. When multiplied by 100, R^2 signifies the percent of the variation from a mean frequency that is common to both short and long-term distributions. In Figure 24, for example, 99% of the variation among 1-year joint frequencies can be predicted based on measured long-term frequencies, while only 1% is attributed to random, year-to-year fluctuations and/or measurement error. In Figure 26, only 11% of the variation at Douglas can be explained by the observed wind patterns at Casper.

Linear correlation produces Pearson's correlation coefficient R, based on the assumption of normally distributed data. The normality assumption can be relaxed by ranking the data and computing Spearman's correlation coefficient, a method commonly applied to nonparametric data. The Casper wind speed comparison yields a Pearson's R of 0.992 and a Spearman's R of 0.964. The Casper wind direction comparison yields a Pearson's R of 0.996 and a Spearman's R of 0.990. Therefore, the assumption of normally distributed data does not compromise the results. Appendix A shows that the Spearman's and Pearson's coefficients are typically similar for wind frequency distributions.

Figure 24 – Casper Short and Long-Term Joint Frequency Distributions

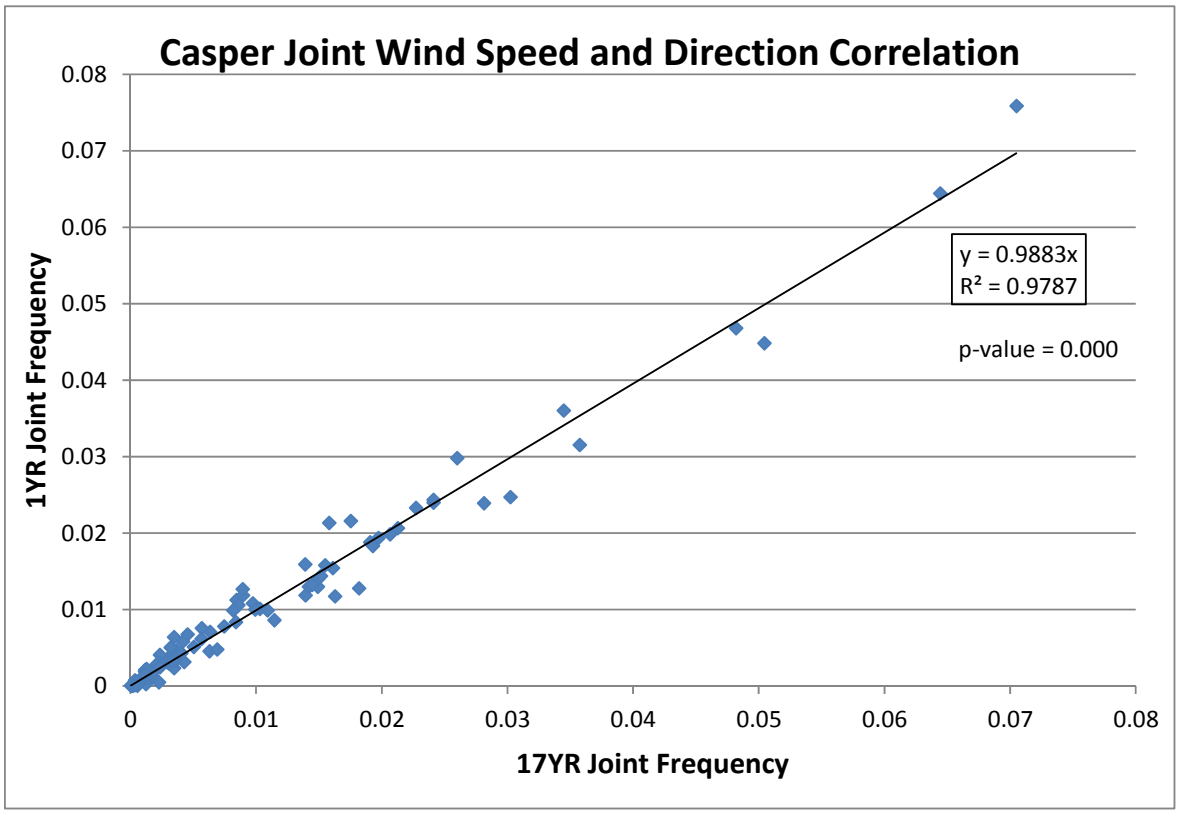

Figure 25 – Douglas Airport Short and Long-Term Joint Frequency Distributions

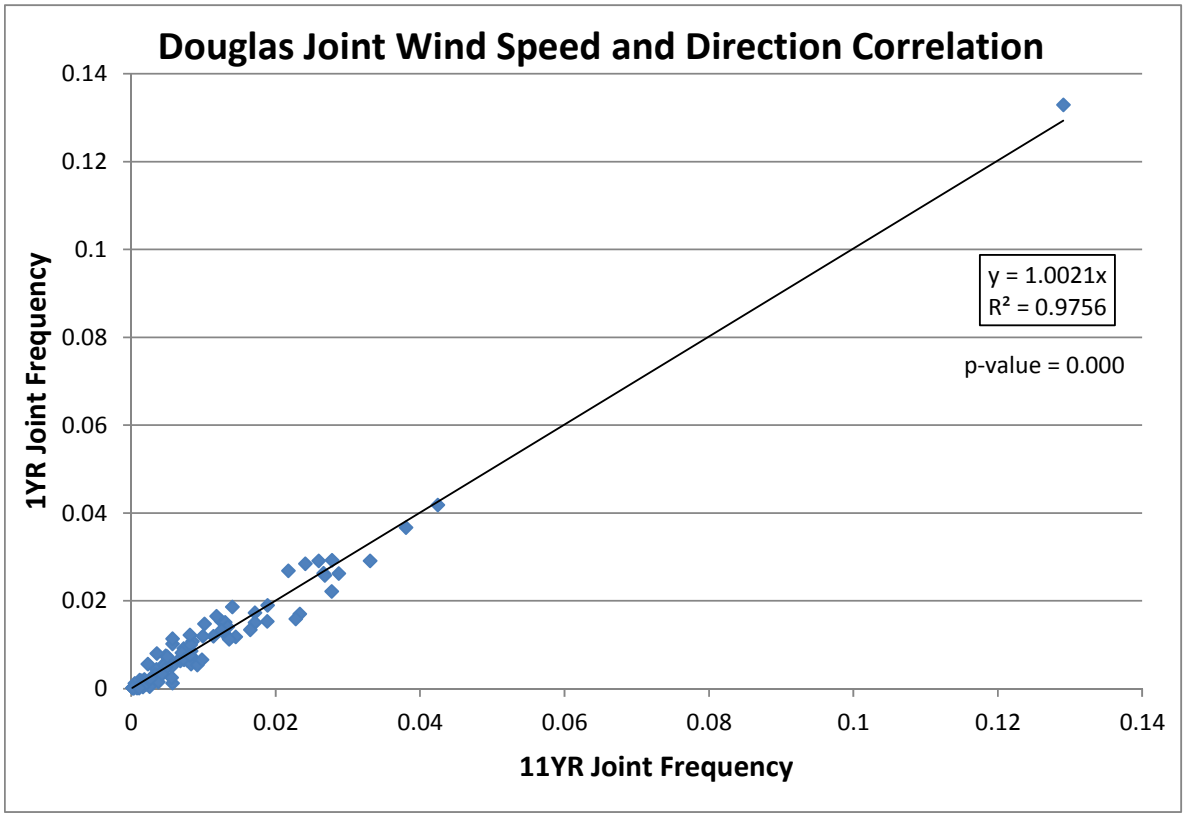

Figure 26 – Douglas and Casper Long-Term Joint Frequency Distributions

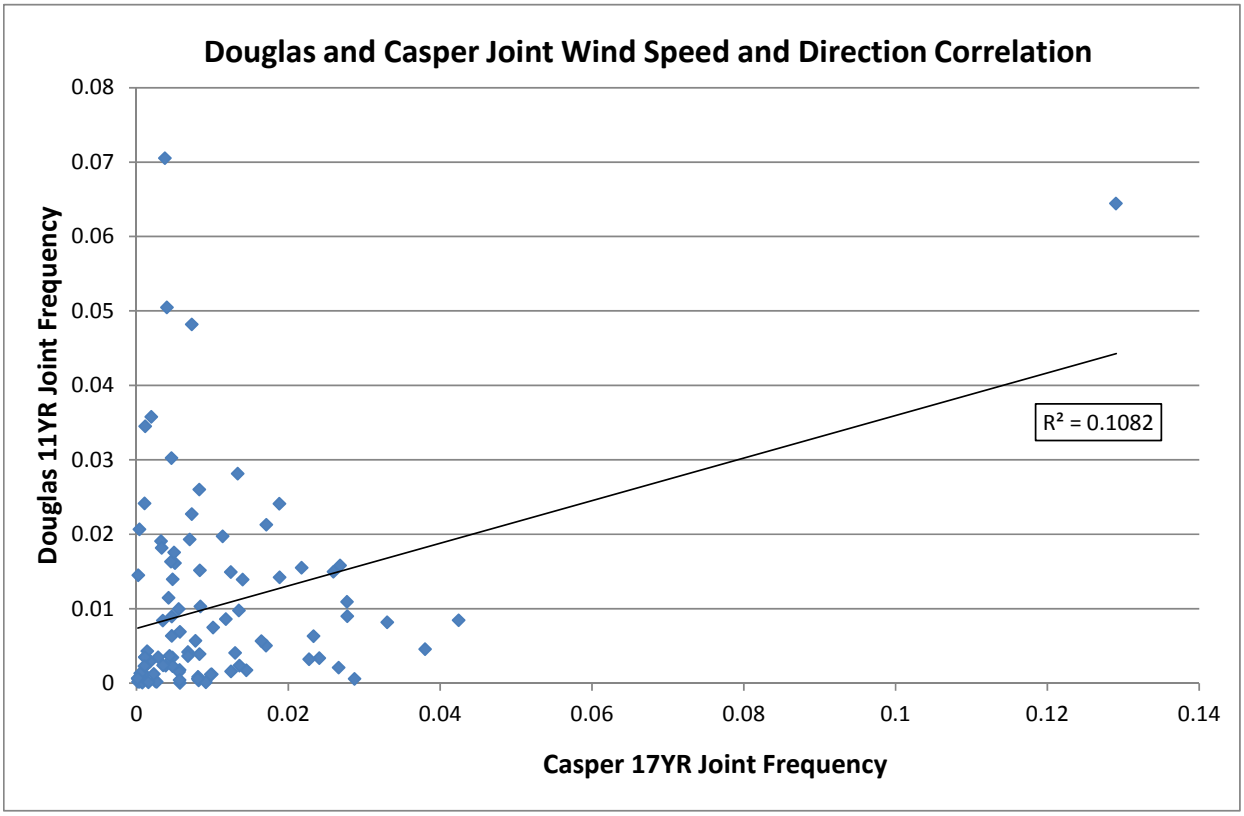

4.8 Conclusion

In fulfillment of NRC guidelines, the combination of visual evidence, summary statistics, linear correlation and hypothesis testing provides a comprehensive demonstration of long-term representativeness of baseline meteorological data at the Ludeman ISR Project site. For the Casper Airport site, the baseline year of hourly wind data are statistically no different than the previous 17 years of data. This conclusion is supported by graphical analyses and by two statistical tests, which have been jointly applied by others to categorize meteorological data (Lowther 1991):

1. χ^2 test (with the phi coefficient to adjust for large sample size)
2. Linear correlation coefficient R (or coefficient of determination R^2)

Table 6 summarizes the test results from Casper wind data. For wind speed, wind direction, and joint frequency distributions, all relevant statistical tests infer the absence of a significant difference between short and long term data.

Table 6 – Summary of Statistical Analysis of Frequency Distributions at Casper

17-Yr vs. 1-Yr Frequency Distributions	Statistical Method						Overall Conclusion
	χ^2 at 8,760 hrs.	Ø-Coeff.	χ^2 at 1,000 hrs.	Ø-Coeff.	Linear Regress. R^2	p-value for R^2	
Wind Speed	48.96	0.07	5.59	0.07	0.983	0.000	No statistical difference
Wind Direction	39.70	0.07	4.53	0.07	0.988	0.000	No statistical difference
Joint Wind Speed and Wind Direction	N/A	N/A	N/A	N/A	0.979	0.000	No statistical difference

The χ^2 test gives a yes/no answer: either the computed statistic results in 95% confidence in a significant difference, or it does not. Linear regression supplies the best measure of the degree of similarity between short-term and long-term wind speed, wind direction and joint frequency distributions. It is uniquely suited to testing joint wind speed and direction frequencies due to the large number of categories.

Casper is considered to be representative of the Ludeman site due to its proximity, similar elevation, comparable terrain, relationship to the east-west trending mountain range to the south, and susceptibility to the same regional climatological factors. With the above demonstration of baseline-year representativeness of long-term wind conditions at Casper, it is reasonable to conclude that baseline-year monitoring at Ludeman also represents the long-term.

5.0 References

AUC 2012, USNRC License Application, Reno Creek ISR Project, Technical Report, Section 2.5, September, 2012 .

Brooks 1978, Handbook of Statistical Methods in Meteorology, C. E. P. Brooks and N. Carruthers, Reprint of 1953 Edition, 1978.

Coffin 1996, Consolidated Statistical Background Papers, U.S. Air Force Climatology Center, Charles R. Coffin, November 1996

EPA 2000, Meteorological Monitoring Guidance for Regulatory Modeling Applications, EPA-454/R-99-005, February 2000

Gardiner 1979, Analysis of Frequency Distributions, Concepts and Techniques in Modern Geography, V. Gardiner & G. Gardiner, 1979.

IML 2015, Meteorological Monitoring Database for Ludeman ISR Project, IML Air Science, Period of Record January, 2014 through February, 2015.

Lowther 1991, RTNEPH Total Cloud Cover Validation Study, Capt Ronald P. Lowther, Mr. Mark T. Surmeier, Capt Richard W. Hartman, Mr Charles R. Coffin, Capt Anthony J. Warren, November 1991.

NCDC 2015, National Climatic Data Center, Quality Controlled Local Climatological Data, accessed 2/19/2015. http://cdo.ncdc.noaa.gov/qclcd/QCLCD?prior=N

NRC 2011, NU-REG 1475, Revision 1, Applying Statistics, March 2011.

NRC 2013, Technical Report - Request for Additional Information, Uranium One Americas, SUA-1341 License Amendment, Ludeman Project, ML12352A030, January 15, 2013.

NRC 2014, Public Meeting Summary, New Request for Additional Information (RAI) - Meteorology, ML14099A027, April 10, 2014.